ISSN 1110-1555

BULLETIN

FACULTY OF SCIENCE

ZAGAZIG UNIVERSITY

18 (2)

December (1996)

Bull.Fac.Sci., Zagazig Univ., 18 (2) 258 - 273 December 1996

APPLICATION OF THE CORE-CORRECTED GLAUBER APPROXIMATION TO POSITRON-ION SCATTERING: II. $e^+ - Be^+$ and $e^+ - Mg^+$ INELASTIC SCATTERING

Zahran E. H. [1], Abdel-Raouf M. A. [2],

Saad A. A.[1], Ramadan H. H. [3]and El-Sakka A. G. [4]

1. Department of Natural and Mathematical Sciences, Faculty of Engineering in Shobra, Zagazig University (Banha - Branch).
2. Department of Physics, Faculty of Science, University of Qatar, Doha, Qatar.
3. Department of Physics, Faculty of Science, Ain Shams University.
4. Department of Mathematics, Faculty of Science, Ain Shams University.

ABSTRACT

The inelastic collision of positrons with Be^+ *and* Mg^+ *is treated for the first time within the framework of a core-corrected Glauber approximation (CCGA).*

A model potential technique based on the one-valence-electron model of the targets is employed using Clementi-Roetti's wavefunctions and ground-state energies. Wavefunctions of the np excited states are considered as the partial derivatives of the corresponding ground-state wavefunctions. To guarantee consistency np wavefunctions are used for calculating the binding energy of the valence-electrons of the corresponding states.

Differential and total excitation (from ns to np states) cross sections are calculated in an incident energy region ranging from 10 to 100 eV. The resulting inelastic cross sections are compared with those determined by other authors.

Introduction

In paper I, we have treated the elastic collision of positrons with beryllium and magnesium positive ions at intermediate energies using the core-corrected Glauber approximation. In this paper the same technique is extended to the treatment of the inelastic collision of positron with positive ions. Particularly, we are interested in $e^+ - Be^+$ and $e^+ - Mg^+$ inelastic scattering. The wavefunctions of np excited states are considered as partial derivatives of the corresponding ns wavefunctions and employed for calculating the excitation energy of the target ions.

Theory

Following paper I, the scattering amplitude of the inelastic collision of positron with positive ion can be obtained by replacing the φ_v^q's (the wavefunction of valence electron of the target ion) of eq. (I.11) by $\varphi_{v^\cdot}^q$'s which is the wavefunction of the excited ion, we obtain

$$F_{v^\cdot v}^{cc}(\bar{q}) = i k_i \int_0^\infty \varphi_{v^\cdot}^q \left[1 - e^{i\chi_a(b,s)} e^{i\chi_c(b)}\right] \varphi_v^q J_0(\bar{q}b)\, b\, db\, dr \quad (1)$$

To obtain $\varphi_{v^\cdot}^q$, we apply (Gien 1987) the differential operator

$$\hat{D}(\alpha) = \sum_\mu A_\mu (-1)^\mu \frac{\partial^\mu}{\partial(\alpha_\mu)^\mu} \quad (2)$$

to φ_v^q. Thus we have

$$\varphi_{v^\cdot}^q(r_v) = \sum_{p=1}^{m_v^q} \bar{C}_{vp}^q r_v^{k_{vp}^q + 1} e^{-\alpha_{vp}^q r_v} \quad (3)$$

The binding energy of the excited valence electron of the ion q is determined by

$$E_{v^\cdot}^q = \left\langle \varphi_{v^\cdot}^q(r) \left| H_v^q \right| \varphi_{v^\cdot}^q(r) \right\rangle = E_1^{*q} + E_2^{*q} + E_3^{*q}$$

The value of E_1^{*q}, E_2^{*q} and E_3^{*q} are given in the Appendix.

Further analyses allow us to write the scattering amplitude in the form

$$F^{cc}_{v'v}(\bar{q}) = 2\pi i K_i \int_0^\infty J_0(\bar{q}b)\, e^{i\chi_c(b)} db \sum_{p=1}^{m_v^q} \sum_{t=1}^{m_v^q} \bar{C}^q_{pv} \bar{C}^q_{tv} s^{J^q_{pt}+3}$$

$$\cdot \int_0^\infty \cosh^{J^q_{pt}+2} u\, e^{-\alpha^q_{pt} s \cosh u} du$$

$$\cdot \left[1 - \left(\frac{2s}{by}\right)^{i\eta} (1-y^2)^{i\eta+\frac{1}{2}} {}_2F_1(i\eta+\tfrac{1}{2}, i\eta+1, 1; y^2)\right] \qquad (4)$$

This can be integrated numerically over b and s (using Gauss-Lagurre technique) to find its value corresponding to a given momentum transfer $\bar{q}$.

The differential excitation cross-section is obtained by

$$\frac{d\sigma_{v'v}}{d\Omega} = \frac{k_f}{k_i} \left| F^{cc}_{v'v}(\bar{q}) \right|^2 \qquad (5)$$

and the total excitation cross-sections can be calculated by

$$\sigma_{v'v} = \frac{1}{k_i^2} \int_{k_i - k_f}^{k_i + k_f} \bar{q}\, d\bar{q} \int_0^{2\pi} d\varphi \left| F^{cc}_{v'v}(\bar{q}) \right|^2 \qquad (6)$$

Note that k_f^2 is related to E_{ns}, E_{np} and k_i^2 by

$$k_f^2 = E_{ns} - E_{np} + k_i^2 , \qquad (7)$$

where E_{ns} is the ground-state energy of the target, E_{np} is its excitation energy (n=2 for Be^+ and n=3 for Mg^+), and $\frac{1}{2} k_i^2$ is the energy of the incident positron (in Hartree atomic units). $\bar{q}$ is related to the scattering angle θ, by the relation

$$\bar{q}^2 = k_i^2 + k_f^2 - 2k_i k_f \cos\theta. \qquad (8)$$

Results and discussions

The inelastic collisions of positrons with Be^{+} and Mg^{+} are treated within the framework of the core-corrected Glauber approximation (CCGA) to calculate the inelastic differential and total cross sections at several energies from E_p = 10 eV to 100 eV. Our results are presented in the following two subsections while distinguish the two processes.

e^{+}-Be^{+} inelastic scattering

We summarize in Table (1) our investigations of the inelastic differential cross sections (in $a_\circ^2$ units) with the momentum transfer $\overline{q}$. The inelastic differential cross sections calculated at certain scattering angle θ (less than 54°) possesses two minima in the energy region 10- 60 eV, while they assume a slowly oscillating behaviour beyond 54°. The inelastic differential cross sections (in $a_\circ^2$ units) of positions scattered by beryllium positive ions are shown in Fig.(1) as a function of the momentum transfer $\overline{q}$ at E_p = 10 and 20 eV. The interesting behaviour is still found in this figure, where the differential cross sections corresponding to E_p = 10 eV are larger than those at E_p = 20 eV. In Fig.(2), four other inelastic differential cross sections are plotted against the momentum transfer $\overline{q}$ at E_p = 30, 40, 50 and 60 eV.

Table (1): The excitation differential cross sections (in $a_\circ^2$) of $e^{+} - Be^{+}$ scattering versus the angle of scattering at different values of the incident energy (E_p) in the energy range 10-100 eV.

E_p / θ	10 eV	20 eV	30 eV	40 eV	50 eV	60 eV	70 eV	80 eV	90 eV	100 eV
1.533	1.180	0.020	0.643	0.007	4.550	23.80	64.90	131.00	223.00	339.00
4.496	1.180	0.019	0.623	0.012	4.730	24.20	65.30	131.00	222.00	334.00
9.110	1.190	0.017	0.543	0.056	5.530	25.90	66.80	130.00	213.00	313.00
15.432	1.210	0.012	0.354	0.307	7.570	29.20	67.30	120.00	183.00	251.00
23.343	1.240	0.003	0.095	1.180	10.60	30.40	57.90	88.50	118.00	143.00
32.667	1.300	0.001	0.021	2.770	11.70	23.40	33.90	41.500	45.50	46.20
43.215	1.380	0.043	0.448	3.770	8.150	10.300	10.400	9.310	7.810	6.260
54.807	1.480	0.210	1.140	2.830	2.810	1.690	0.777	0.320	0.142	0.087
67.276	1.580	0.571	1.390	1.020	0.169	0.031	0.263	0.336	0.199	0.039
80.469	1.680	1.060	1.020	0.062	0.269	0.907	0.992	0.540	0.076	0.084
94.256	1.750	1.490	0.469	0.127	1.000	1.290	0.699	0.055	0.266	1.620
108.518	1.800	1.720	0.122	0.512	1.200	0.821	0.102	0.194	1.350	3.100
123.152	1.840	1.760	0.008	0.728	0.930	0.297	0.012	0.543	1.540	2.600
138.063	1.870	1.690	0.007	0.740	0.612	0.086	0.061	0.467	1.050	1.460
153.155	1.890	1.600	0.030	0.684	0.427	0.039	0.044	0.287	0.611	0.664
168.282	1.900	1.530	0.047	0.641	0.351	0.033	0.022	0.184	0.388	0.330

ig. (3) contains the plots corresponding to the last four values of E_p, amely 70, 80, 90 and 100 eV. The oscillating behaviour of $\frac{d\sigma_{fi}}{d\Omega}$ as function of $\overline{q}$ (or θ) at different values of E_p appears clearly in oth figures. Fig. (3) illustrates that the inelastic differential cross ection falls off rapidly as the incident energy increases.

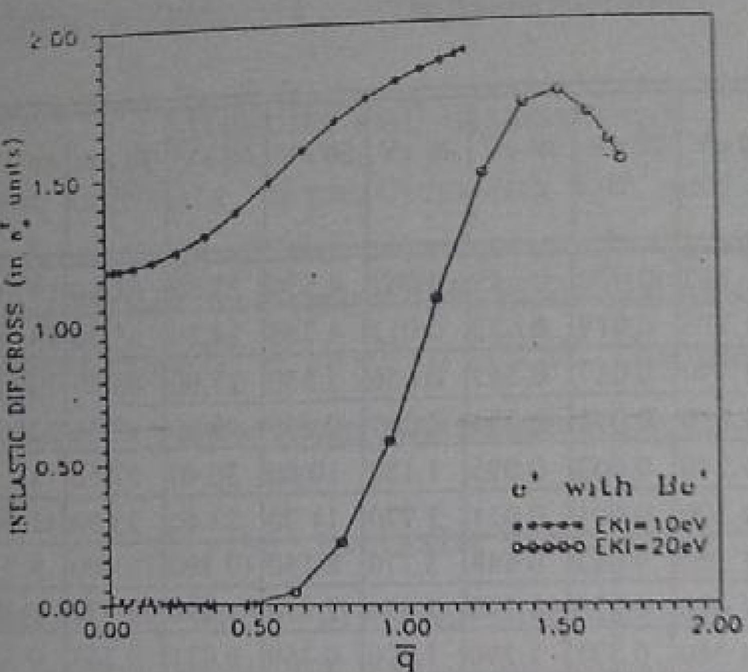

Fig. (1): The excitation differential cross sections (in a_0^2) of $e^+ - Be^+$ scattering as a function of the momentum transfer $\bar{q}$ at the incident energy (E_p) in the energy range 10 and 20 eV.

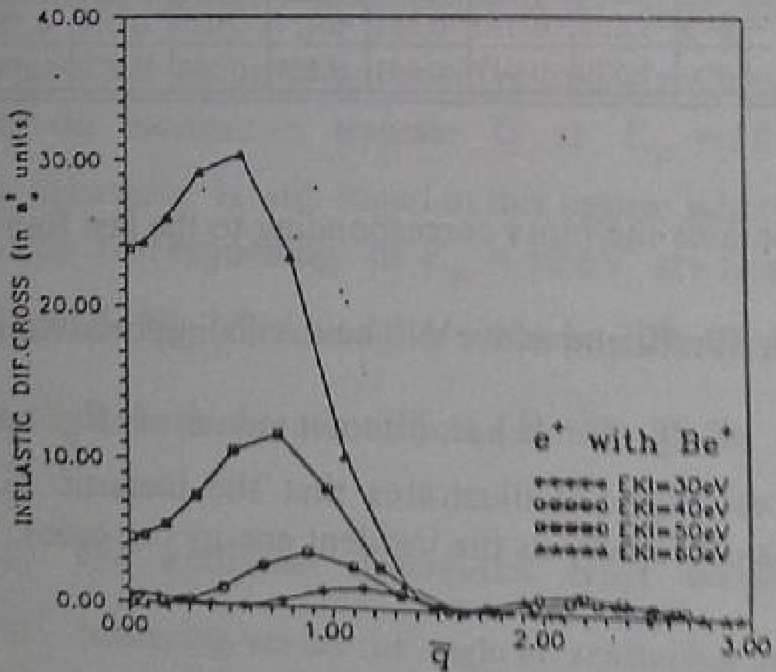

Fig. (2): The excitation differential cross sections (in a_0^2) of $e^+ - Be^+$ scattering as a function of the momentum transfer $\bar{q}$ at the incident energy (E_p) in the energy range 30, 40, 50 and 60 eV.

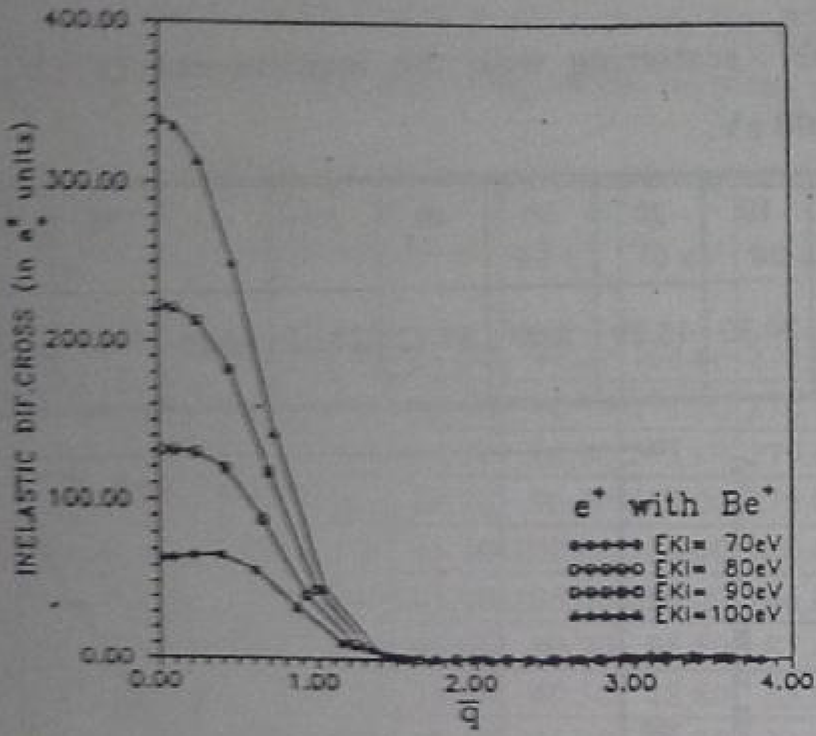

Fig. (3): The excitation differential cross sections (in a_o^2) of $e^+ - Be^+$ scattering as a function of the momentum transfer $\overline{q}$ at the incident energy (E_p) in the energy range 70, 80, 90 and 100 eV.

This behaviour was confirmed by Gien (1987) in his work on e^+-alkali atom scatterings and by Gien and Yan (1990) in their work on positron scattering by metastable hydrogen. The earlier work was treated via core-corrected modified Glauber approximation, while the latter was treated via Glauber approximation.

The results of the total inelastic cross sections are given in Table (2) and displayed in Fig. (4).

Table (2): Variation of the total excitation cross sections (in a_o^2) of $e^+ - Be^+$ scattering with the incident energy (E_p) in the energy range 10-100 eV.

E_p	10	20	30	40	50	60	70	80	90	100
σ_{total}	20.30	13.29	6.00	13.12	28.65	48.25	73.04	103.99	140.21	178.81

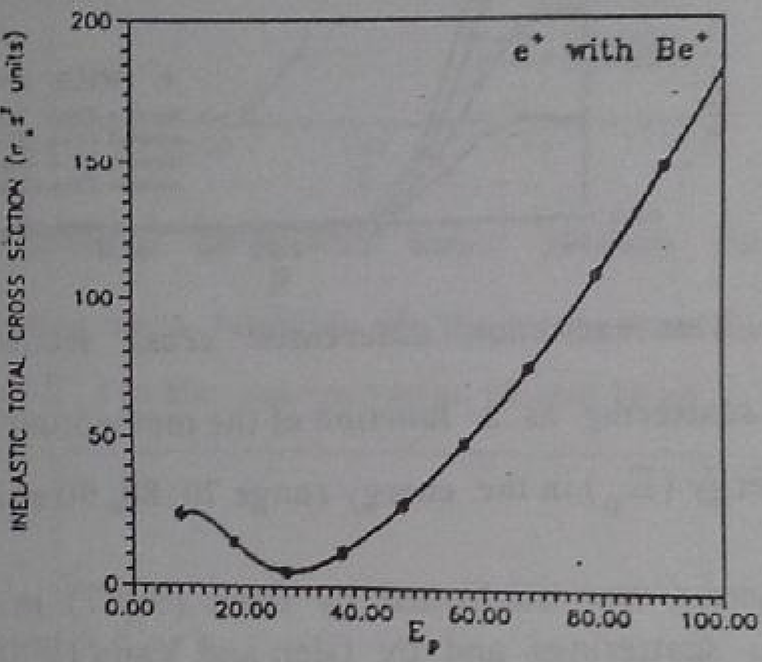

Fig. (4): The total excitation cross section (in a_o^2) of $e^+ - Be^+$ scattering versus the incident energy (E_p) in the energy range 10-100 eV.

$e^+ - Mg^+$ inelastic scattering

In Table (3), we summarize our calculations of the inelastic differential cross sections determined at different values of the scattering angle θ for the collision of positrons with magnesium positive ions. Fig. (5) shows the inelastic differential cross sections (in a_o^2) of positrons with Mg^+ at $E_p = 10$ and 20 eV.

Table (3): The excitation differential cross sections (in a_o^2) of $e^+ - Mg^+$ scattering versus the angle of scattering at the incident energy range 10-100 eV.

θ \ E_p	10 eV	20 eV	30 eV	40 eV	50 eV	60 eV	70 eV	80 eV	90 eV	100 eV
3.137	15.30	25.10	10.20	0.440	14.90	77.20	169.00	274.00	401.00	566.00
7.653	15.20	24.90	9.91	0.342	15.70	78.90	171.00	276.00	400.00	562.00
13.137	15.00	24.10	8.96	0.107	18.30	84.80	178.00	279.00	394.00	540.00
19.827	14.60	22.60	6.98	0.064	24.70	96.50	187.00	275.00	365.00	472.00
27.784	14.00	20.10	4.04	1.430	35.10	108.00	184.00	240.00	285.00	333.00
36.957	13.10	16.40	1.210	5.240	43.90	105.00	150.00	166.00	168.00	172.00
47.236	11.90	12.20	0.004	9.640	43.00	80.70	95.50	87.40	72.90	63.100
58.485	10.50	7.91	0.687	10.90	31.80	49.30	48.80	35.90	23.20	16.100
70.567	9.07	4.46	1.870	8.320	18.40	25.20	21.30	11.90	4.86	1.930
83.352	7.72	2.19	2.280	4.570	8.650	11.50	8.39	3.01	0.32	0.014
96.716	6.54	0.969	1.00	1.800	3.450	5.07	3.35	0.67	0.03	0.536
110.551	5.57	0.420	1.180	0.456	1.250	2.53	1.71	0.15	0.40	1.600
124.756	4.82	0.200	0.630	0.039	0.452	1.53	0.95	0.001	1.37	3.460
139.239	4.27	0.117	0.310	0.012	0.169	0.974	0.40	0.25	2.67	5.370
153.904	3.91	0.087	0.155	0.086	0.060	0.604	0.11	0.66	3.67	6.730
168.608	3.72	0.077	0.093	0.151	0.022	0.410	0.02	0.95	4.18	7.440

From the figure we notice that the inelastic differential cross section calculated at E_p = 20 eV diminishes mush faster than the one determined at E_p = 10 eV. In Fig. (6), the inelastic differential cross sections (measured in a_o^2 units) are shown as functions of the momentum transfer $\overline{q}$, at E_p = 30, 40, 50 and 60 eV. We notice that the cross sections are peaked and the oscillating behaviour still shown up. Fig. (7) contains the plots corresponding to the last four values of E_p, namely 70, 80, 90 and 100 eV.

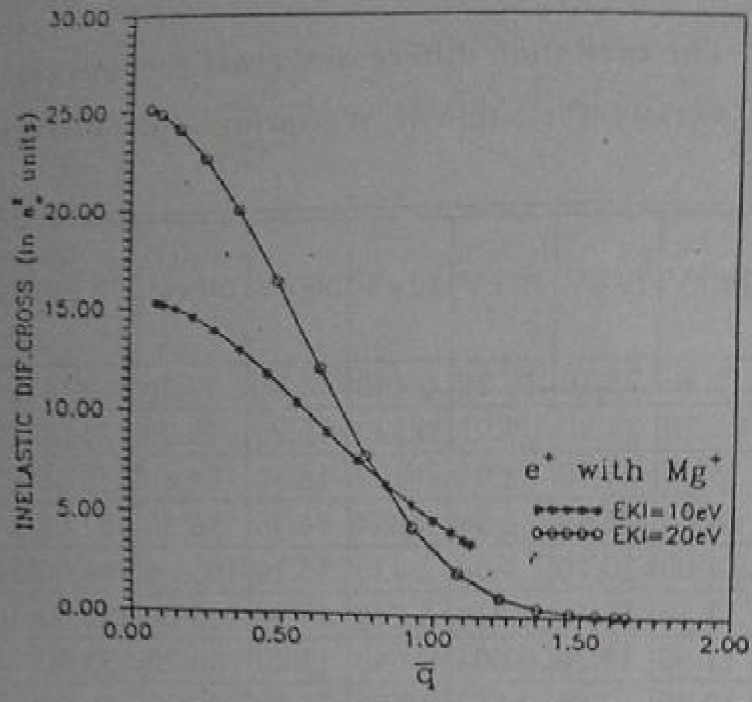

Fig. (5): The excitation differential cross sections (in a_o^2) of $e^+ - Mg^+$ scattering as a function of the momentum transfer $\overline{q}$ at the incident energy (E_p) in the energy range 10 and 20 eV.

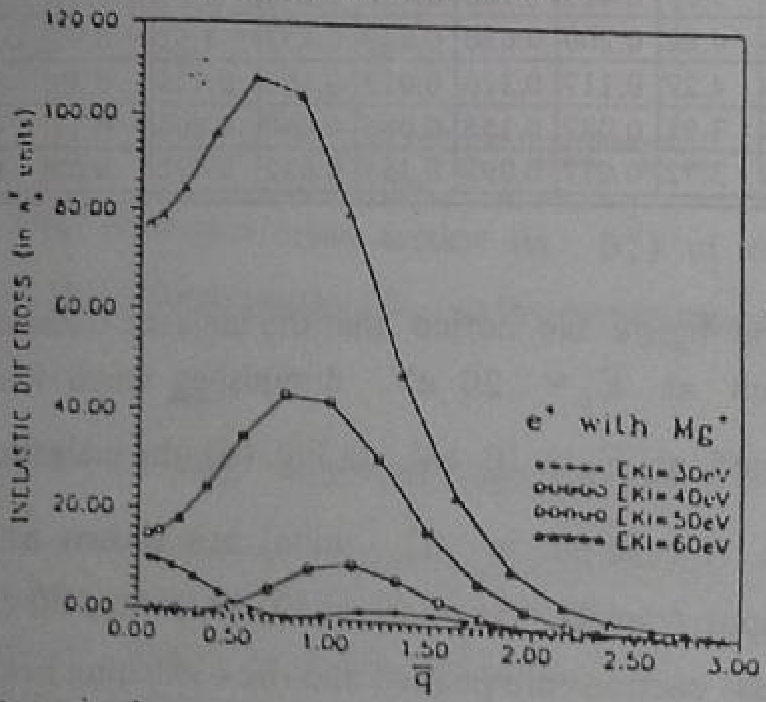

Fig. (6): The excitation differential cross sections (in a_o^2) of $e^+ - Mg^+$ scattering as a function of the momentum transfer $\overline{q}$ at the incident energy (E_p) in the energy range 30, 40, 50 and 60 eV.

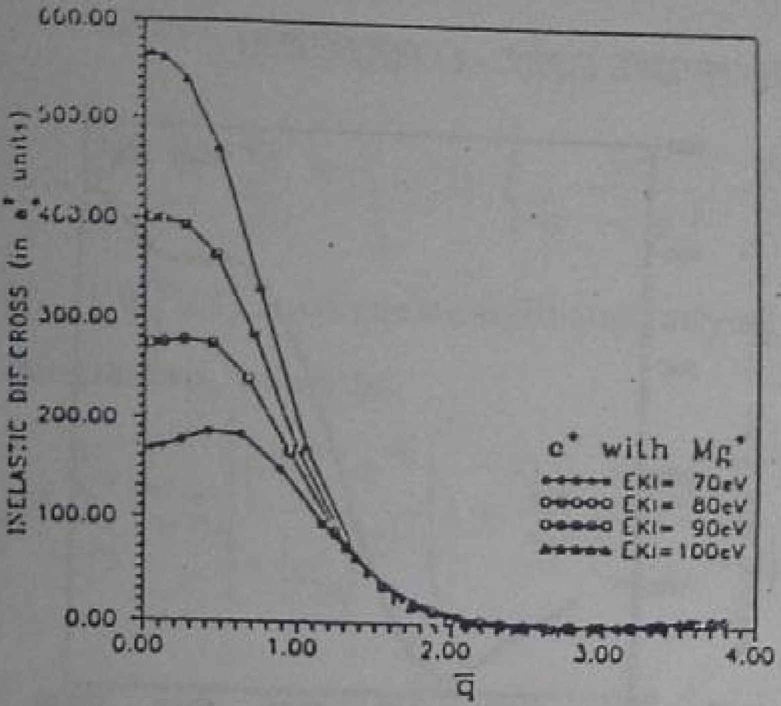

Fig. (7): The excitation differential cross sections (in a_0^2) of $e^+\_Mg^+$ scattering as a function of the momentum transfer $\overline{q}$ at the incident energy (E_p) in the energy range 70, 80, 90 and 100 eV.

There, we see that the cross sections are sharply peaked in the forward direction as the energy increases, and fall off somewhat faster as the momentum $\overline{q}$ (or the scattering angle θ) increases. This agrees with the results of Gien and Yan (1990) for the collision of positrons with metastable hydrogen atoms obtained using Wallace and Glauber approximations (1971). The total inelastic cross sections of $e^+ - Mg^+$ scattering are tabulated with the incident energy in Table (4), and displayed in Fig. (8).

Table (4): Variation of the total excitation cross sections (in a_0^2) of $e^+\_Mg^+$ scattering with the incident energy (E_p) in the energy range 10-100 eV.

E_p	10	20	30	40	50	60	70	80	90	100
σ_{total}	85.54	54.00	16.85	43.15	156.90	310.35	389.37	401.09	418.67	467.51

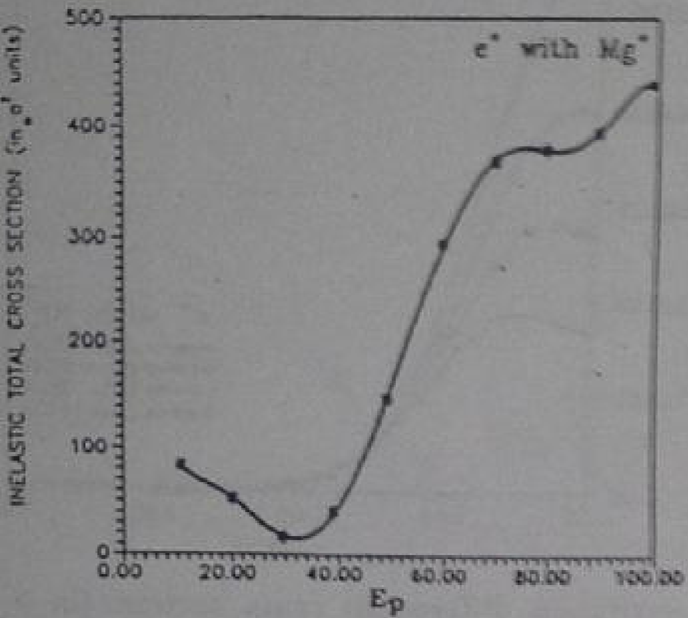

Fig. (8): The total excitation cross section (in a_0^2) of $e^+ - Mg^+$ scattering versus the incident energy (E_p) in the energy range 10-100 eV.

Conclusion

From the results presented in the previous sections, we introduce the following remarks:

1) The oscillatory behaviour of the inelastic differential cross sections calculated at the intermediate energy region supports possible resonances in this region.

2) The total inelastic cross sections increase steadily with the energy above 30 eV. This is attributed to the fact that the interaction potential between the positrons and target ions are mainly repulsive.

Appendix

This Appendix is devoted to the representation of the core potentials, $V_{c\ Coul}(r)$ (eq. 3) and the three parts of the binding energies of the np states of the targets, (eq. 33b), (in a. us.), in closed or simpler forms. From the definition of $V_{c\ Coul}(r)$, we have

$$V^{q}_{Coul}(r) = \sum_{j=1}^{M^{q}} N^{q}_{j} \left\langle \varphi^{q}_{j}(r_{i}) \left| \frac{1}{|r - r_{i}|} - \frac{1}{r} \right| \varphi^{q}_{j}(r_{i}) \right\rangle.$$

Substituting $\left| \varphi^{q}_{j}(r) \right\rangle$ from equation (9) and carrying out the angular and radial integrations, we obtain

$$V^{q}(r) = \sum_{j=1}^{M_{q}} N^{q}_{j} \sum_{p,s=1}^{m^{q}_{j}} \overline{C}^{q}_{jp} \overline{C}^{q}_{js} \left[\frac{(J^{q}_{ps})!\, e^{-\alpha^{q}_{ps} r}}{r (\alpha^{q}_{ps})^{J^{q}_{ps}+1}} \left(1 + \sum_{i=1}^{J^{q}_{ps}-1} \frac{i (\alpha^{q}_{ps} r)^{J^{q}_{ps}-i}}{J^{q}_{ps} (J^{q}_{ps} - i)!} \right) + \sum_{n>0}^{\infty} C^{n} I_{n} \right],$$

$$I_{n} = \frac{(J^{q}_{ps} + n)!}{r^{n+1} (\alpha^{q}_{ps})^{J^{q}_{ps}+n+1}} \left[e^{-\alpha^{q}_{ps} r} - 1 \right] + \frac{(J^{q}_{ps} + n)!\, e^{-\alpha^{q}_{ps} r}}{r^{n+1} (\alpha^{q}_{ps})^{J^{q}_{ps}+n+1}} \sum_{i=J^{q}_{ps}-n}^{J^{q}_{ps}+n-1} \frac{(r\alpha^{q}_{ps})^{J^{q}_{ps}-i}}{(J^{q}_{ps} + n - i)!}$$

$$+ \frac{e^{-\alpha^{q}_{ps} r}}{r^{n+1} (\alpha^{q}_{ps})^{J^{q}_{ps}+n+1}} \sum_{i=1}^{J^{q}_{ps}-n-1} \left(\frac{(J^{q}_{ps} + n)!}{(J^{q}_{ps} + n - i)!} - \frac{(J^{q}_{ps} + n - 1)!}{(J^{q}_{ps} + n - 1 - i)!} \right) (r\alpha^{q}_{ps})^{J^{q}_{ps}+n-i}$$

where $J^{q}_{ps} = k^{q}_{js} + k^{q}_{jp}$ and $\alpha^{q}_{ps} = \alpha^{q}_{js} + \alpha^{q}_{jp}$. The constants C^{n} depend on the orders of the spherical harmonics of the Slater basis functions as well as the degree of the Legendre polynomial due to the expansion of the two body potential (see Condon and Shortley 1970 [pp 178-180]). The three parts of the excitation energy np, (see eq. 33), are determined (in a. us.) by

$$E^{*q}_{1} = \left\langle \varphi^{q}_{v^{*}}(r_{v}) \left| -\frac{1}{2} \nabla^{2}_{r_{v}} - \frac{Z_{eff}}{r_{v}} \right| \varphi^{q}_{v^{*}}(r_{v}) \right\rangle$$

$$= \frac{-1}{2} \sum_{p=1}^{m^{q}_{v}} \sum_{t=1}^{m^{q}_{v}} \overline{C}^{q}_{pv} \overline{C}^{q}_{tv} \left\{ \overline{k}^{q}_{tv} (\overline{k}^{q}_{tv} + 1) \frac{(\overline{J}^{q}_{pt} - 2)!}{(\alpha^{q}_{pt})^{\overline{J}^{q}_{pt}-1}} \right.$$

$$-2\left(\alpha^q_{tv}\left(\bar{k}^q_{tv}+1\right)-Z_{eff}\right)\frac{\left(\bar{J}^q_{pt}-1\right)!}{\left(\alpha^q_{pt}\right)^{\bar{J}^q_{pt}}}+\left(\alpha^q_{tv}\right)^2\frac{\left(\bar{J}^q_{pt}\right)!}{\left(\alpha^q_{pt}\right)^{\bar{J}^q_{pt}+1}}\Bigg\}$$

$$E^{*q}_2 = \left\langle \varphi^q_{v^*}(r)\middle| V_{c\ coul}(r)\middle|\varphi^q_{v^*}(r)\right\rangle$$

$$= -\sum_{j=1}^{M_q} N^q_j \sum_{p,t=1}^{m^q_j} \bar{C}^q_{pv}\bar{C}^q_{tv}\sum_{\mu,\nu=1}^{m^q_j}\bar{C}^q_{\mu j}\bar{C}^q_{\nu j}\Bigg\{\frac{\left(J^q_{\mu\nu}\right)!}{\left(\alpha^q_{\mu\nu}\right)^{J^q_{\mu\nu}+1}}\frac{\left(\bar{J}^q_{pt}-1\right)!}{\left(\alpha^q_{pt}+\alpha^q_{\mu\nu}\right)^{\bar{J}^q_{pt}}}$$

$$+\frac{\left(J^q_{\mu\nu}\right)!}{\left(\alpha^q_{\mu\nu}\right)^{J^q_{\mu\nu}+1}}\sum_{i=1}^{J^q_{\mu\nu}-1}\frac{i\left(\alpha^q_{\mu\nu}\right)^{J^q_{\mu\nu}-i}}{\left(J^q_{\mu\nu}\right)\left(J^q_{\mu\nu}-i\right)!}\frac{\left(\bar{J}^q_{pt}+J^q_{\mu\nu}-1-i\right)!}{\left(\alpha^q_{pt}+\alpha^q_{\mu\nu}\right)^{\bar{J}^q_{pt}+J^q_{\mu\nu}-i}}$$

$$+\sum_{n>0}^{\infty}C^n\Bigg[\frac{\left(J^q_{\mu\nu}+n\right)!}{\left(\alpha^q_{\mu\nu}\right)^{J^q_{\mu\nu}+n+1}}\left(\frac{\left(\bar{J}^q_{pt}-1-n\right)!}{\left(\alpha^q_{pt}+\alpha^q_{\mu\nu}\right)^{\bar{J}^q_{pt}-n}}-\frac{\left(\bar{J}^q_{pt}-1-n\right)!}{\left(\alpha^q_{pt}\right)^{\bar{J}^q_{pt}-n}}\right)$$

$$+\frac{\left(J^q_{\mu\nu}+n\right)!}{\left(\alpha^q_{\mu\nu}\right)^{J^q_{\mu\nu}+n+1}}\sum_{i=J^q_{\mu\nu}-n}^{J^q_{\mu\nu}+n+1}\frac{\left(\alpha^q_{\mu\nu}\right)^{J^q_{\mu\nu}+n-i}}{\left(\bar{J}^q_{pt}+n-i\right)!}\frac{\left(\bar{J}^q_{pt}+J^q_{\mu\nu}-1-i\right)!}{\left(\alpha^q_{pt}+\alpha^q_{\mu\nu}\right)^{\bar{J}^q_{pt}+J^q_{\mu\nu}-i}}$$

$$+\sum_{i=1}^{J^q_{\mu\nu}-n-1}\frac{1}{\left(\alpha^q_{\mu\nu}\right)^{i+1}}\left(\frac{\left(\bar{J}^q_{\mu\nu}+n\right)!}{\left(\bar{J}^q_{\mu\nu}+n-i\right)!}-\frac{\left(\bar{J}^q_{\mu\nu}-n-1\right)!}{\left(J^q_{\mu\nu}-n-1-i\right)!}\right)\frac{\left(\bar{J}^q_{pt}+J^q_{\mu\nu}-1-i\right)!}{\left(\alpha^q_{pt}+\alpha^q_{\mu\nu}\right)^{\bar{J}^q_{pt}+J^q_{\mu\nu}-i}}\Bigg]$$

$\bar{J}^q_{pt} = \bar{k}^q_{jt}+\bar{k}^q_{jp}, \bar{k}^q_{jt} = k^q_{jt}+1, \bar{k}^q_{jp} = k^q_{jp}+1,$
$J^q_{\mu\nu} = k^q_{j\mu}+k^q_{j\nu}$ and $\alpha^q_{\mu\nu} = \alpha^q_{j\mu}+\alpha^q_{j\nu})$

$$E_3^{*q} = \left\langle \varphi_{v^*}^{q}(r) \middle| V_{c\ ex}(r) \middle| \varphi_{v^*}^{q}(r) \right\rangle$$

$$= \sum_{j=1}^{M_q} \sum_{\mu=1}^{m_j^q} \sum_{v=1}^{m_j^q} \sum_{t=1}^{m_j^q} \sum_{p=1}^{m_j^q} \overline{C}_{\mu v}^{q} \overline{C}_{jv}^{q} \overline{C}_{vt}^{q} \overline{C}_{jp}^{q} \left\{ \sum_{i=J_{tv}^q-n}^{J_{tv}^q+n} \frac{\left(J_{tv}^q+n\right)!}{\left(J_{tv}^q+n-i\right)!\left(\alpha_{tv}^q\right)^{i+1}} \right.$$

$$\cdot \frac{\left(\overline{J}_{\mu v}^q + J_{tv}^q - i - 1\right)!}{\left(\alpha_{\mu p}^q + \alpha_{tv}^q\right)^{\overline{J}_{\mu p}^q + J_{tv}^q - i}} + \sum_{i=1}^{J_{\mu v}^q - n - 1} \left(\frac{\left(J_{tv}^q+n\right)!}{\left(J_{tv}^q+n-i\right)!} - \frac{\left(J_{tv}^q-n-1\right)!}{\left(J_{tv}^q-n-1-i\right)!} \right)$$

$$\left. \cdot \frac{1}{\left(\alpha_{tv}^q\right)^{i+1}} \frac{\left(\overline{J}_{\mu v}^q + J_{tv}^q - i - 1\right)!}{\left(\alpha_{\mu p}^q + \alpha_{tv}^q\right)^{\overline{J}_{\mu p}^q + J_{tv}^q - i}} \right\}$$

References

Abdel - Raouf M. A. , (1988), Chem. Phys. 123 , 375.

Abdel - Raouf M. A. , (1988), J. Phys. B : At. Mol. Opt. Phys. 21 , 2331.

Abdel-Raouf M. A. (1989), IL Nuovo Cimento 433-453.

Abdel-Raouf M. A. (1989), IL Nuovo Cimento 791-797.

Brian K. T. and Victor F., (1976), Phys. Rev. A 13 , 2004.

Clementi E. and Roetti C.,(1974),At. Data Nucl. Data Tables 14 , 177.

Condon E. U. and Shortley G. H. (1970) The Theory of Atomic Spectra (Cambridge: Cambridge University Press)

Franco V. , (1968) Phys. Rev. Let. 20, 709 (And Reference therein).

Gien T. T. , (1987), Phys. Rev. A , 35 2026.

Gien T. T., (1988), J. Phys. B : At. Mol. Opt. Phys. 21 , 3767.

Gien T. T. and Yan Z. C., (1990) Phys. Rev. A , 42 , No. 5, 3121.

Glauber R. G. (1959), in: Lecture in Theoretical physics, vol. I, ed. w. E. Brittin (Interscience, New York,) p. 315.

Tai H., Bassel R. H., Gerjuoy E. and Franco V., (1970), Phys. Rev. A 1 , 1819 (And Reference therein).

Wallace S. J., (1971), Phys. Rev. Lett. 27, 622.

تطبيق طرق جلاوبر التقريبية المصححة على استطارة البوزيترون بواسطة أيون موجب:

II. الاستطارة غير المرنة للبوزيترون بواسطة Be^+ و Mg^+

عماد حسن زهران[1]
محمد أسعد عبد الرءوف[2]
عبد الرحمن على سعد[1]
حسن حسن رمضان[3]
أحمد جلال السقا[4]

١- قسم العلوم الطبيعية والرياضية- كلية الهندسة بشبرا.-جامعة الزقازيق (فرع بنها)
٢- قسم الفيزياء- كلية العلوم - جامعة قطر - الدوحة - قطر
٣- قسم الفيزياء - كلية العلوم - جامعة عين شمس
٤- قسم الرياضيات - كلية العلوم - جامعة عين شمس

مستخلص

لقد تم معالجة التصادمات غير المرنة للبوزيترونات مع Be^+ و Mg^+ باستخدام تقريب جلاوبر المصحح. وقد أستخدم نموذج للجهد يعتمد على إلكترون التكافؤ المفرد للأهداف يعتمد على دوال الحالة لكلمنتي و روتي مع إعتبار مستويات الطاقة الأرضية المناظرة لها. وتم إعتبار دوال الحالات المثارة (np) كتفاضلات جزئية لدوال الحالات الأرضية المناظرة. وتم حساب طاقات الربط للإلكترونات المدارية المؤثرة فى هذا التفاعل بإستخدام ذات الحالات المثارة. وقد تم حساب المقاطع المستعرضة التفاضلية والمثارة الكلية فيما بين الحالات (ns-np) فى مدى للطاقة يتراوح بين ١٠ إلى ١٠٠ إلكترون فولت. وأجريت مقارنات للمقاطع المستعرضة للإستطارة غير المرنة لنتائج هذه الدراسة مع بعض النتائج البحثية الأخرى.

مجلة كلية العلوم

جامعة الزقازيق

١٨(٢)

ديسمبر ١٩٩٦

رقم الإيداع بدار الكتب والوثائق القوميه ٧٨٢ / ١٩٩٣